Polymer 50 (2009) 6245–6251

Contents lists available at ScienceDirect

Polymer

journal homepage: www.elsevier.com/locate/polymer

Synthesis and characterization of phenylene-thiophene all-conjugated diblock copolymers

Shupeng Wu [a,b], Laju Bu [a,b], Li Huang [a,b], Xinhong Yu [a], Yanchun Han [a], Yanhou Geng [a,*], Fosong Wang [a]

[a] State Key Laboratory of Polymer Physics and Chemistry, Changchun Institute of Applied Chemistry, Chinese Academy of Sciences, Changchun 130022, PR China
[b] Graduate School of Chinese Academy of Sciences, Beijing 100049, PR China

ARTICLE INFO

Article history:
Received 3 July 2009
Received in revised form
24 October 2009
Accepted 2 November 2009
Available online 5 November 2009

Keywords:
GRIM polymerization
All-conjugated block copolymer
Microphase separation

ABSTRACT

Grignard metathesis (GRIM) polymerization for all-conjugated diblock copolymers comprising poly (2,5-dihexyloxy-1,4-phenylene) (PPP) and poly(3-hexylthiophene) (P3HT) blocks were systematically studied with LiCl as additive and 1,2-bis (diphenylphosphino) ethane nickel dichloride (Ni(dppe)Cl_2) or 1,3-bis(diphenylphosphino) propane nickel dichloride (Ni(dppp)Cl_2) as catalyst. It was found that the addition order of the monomers was crucial for the success of copolymerization. With the monomer addition in the order of phenyl and then thienyl Grignard reagents, all-conjugated PPP-*b*-P3HT diblock copolymers with different block ratios were successfully synthesized. In contrast, the inverted addition order only afforded a mixture containing both block copolymers and deactivated or end-capped homopolymers. Mass spectroscopic analysis indicates that the effect of the addition order of the monomers on copolymerization is attributed to the low efficiency of intramolecular Ni transfer from thiophene to phenylene units. The resulting PPP-*b*-P3HT diblock copolymers were characterized by differential scanning calorimetry (DSC) and atomic force microscopy (AFM). It was found that both PPP and P3HT blocks in the copolymers were crystalline, and microphase separation between them took place, as indicated by two endothermal transitions corresponding to the melting of PPP and P3HT blocks, respectively. These unique properties may render PPP-*b*-P3HT diblock copolymers potential applications in optoelectronics.

© 2009 Elsevier Ltd. All rights reserved.

1. Introduction

Conjugated polymers are very attractive as advanced materials nowadays due to their applications in optoelectronic devices [1–3], and detail studies have shown that nanostructures in solid state are crucial for their optoelectronic properties [4,5]. On the other hand, it is well-known that block copolymers with well-defined chemical structures can form controllable nanostructures via microphase separation [6,7]. However, it is rather difficult to synthesize well-defined all-conjugated block copolymers for lack of appropriate polymerization methods [7].

Recently, a new "quasi-living" polymerization method named Grignard metathesis (GRIM) polymerization was developed by McCullough and Yokozawa [8–11]. Using this method, well-controlled conjugated polymers including polythiophenes (PThs) with various functional groups [12,13], poly(*p*-phenylene) (PPP) [14], polyfluorene [15,16], polypyrrole [16,17] and polycarbazole [16] have been successfully prepared. Molecular weights of the resulting polymers can be tuned by changing the molar ratio of monomer to catalyst, and meanwhile, their polydispersity indices (PDI = weight-average molecular weight/number-average molecular weight (M_w/M_n)) are much narrower than those of the conjugated polymers synthesized by step-growth organometallic polycondensations [8–17]. By using appropriate catalyst, polymer brushes have also be prepared via surface initiated GRIM polymerization [18–20]. One of the advantages of GRIM polymerization is that desired terminal groups can be introduced via efficient end-capping, which allows preparation of macromonomers [21,22] or macroinitiators [23–32] for synthesis of polythiophene (PTh)-based rod-coil diblcok copolymers, such as poly(3-hexylthiophene)-*block*-polyacrylate (P3HT-*b*-PA) [26,31,32] and poly(3-hexylthiophene)-*block*-polystyrene (P3HT-*b*-PS) [21,22,25,27,30]. Some of these copolymers show nanofibrillar morphologies in solid state due to microphase separation, which lead to high conductivities despite the presence of the insulating block [27–30,32]. All-conjugated diblock copolymers comprising thiophene units with different side chains were also successfully synthesized by GRIM polymerization [10,33–38], and these copolymers can also form microphase-separated nanostructures [34,35]. It can be postulated that all-conjugated diblock copolymer comprising different aryl

* Corresponding author. Tel.: +86 431 5262918; fax: +86 431 5685653.
E-mail address: yhgeng@ciac.jl.cn (Y. Geng).

0032-3861/$ – see front matter © 2009 Elsevier Ltd. All rights reserved.
doi:10.1016/j.polymer.2009.11.001

units can combine functions of different conjugated polymers, and meanwhile should possess capability of nanostructure formation like aforementioned block copolymers. Considering the importance of PThs as high performance organic semiconductors, it is very attractive to prepare PTh-based all-conjugated block copolymers with other conjugated blocks. Recently, Yokozawa et al. first reported that GRIM method could be used in the synthesis of poly(2,5-dihexyloxy-*p*-phenylene)-*block*-poly(3-hexylthiophene) (PPP-*b*-P3HT) [39]. In the current paper, we systematically studied the synthesis of PPP-*b*-P3HT block copolymers with different block ratios and their photophysical and thermal properties.

2. Experimental section

2.1. Materials

Tetrahydrofuran (THF) was distilled over sodium/benzophenone. Isopropylmagnesium chloride (^{i}PrMgCl, 2.0 M solution in THF, Aldrich), *t*-butylmagnesium chloride (^{t}BuMgCl, 1.7 M solution in THF, Acros), Ni(dppp)Cl_2, (1,3-bis(diphenylphosphino) propane nickel dichloride, Pacific ChemSource, Inc., Zhengzhou, China, 98%), and Ni(dppe)Cl_2 (1,2-bis (diphenylphosphino) ethane nickel dichloride, Pacific ChemSource Inc., Zhengzhou, China, 98%) were used as received without further purification. Lithium chloride (LiCl, Acros, 99%) was heated at 130 °C in vacuum for 5 h prior to use. Compounds 2,5-dibromo-1,4-dihexyloxybenzene (**1**) [14], 1,4-dioctyloxybenzene [40], 1,4-dipentyloxybenzene [41] and 2,5-dibromo-3-hexylthiophene (**2**) [10] were synthesized according to the references. Their purities are all above 99.5% according to GC measurements.

2.2. Instrumentation and measurements

^{1}H NMR spectra were recorded on a Bruker AV 300 spectrometer at 300 MHz in $CDCl_3$ with tetramethylsilane (TMS) as an internal reference. Gas chromatography (GC) measurements were carried out on an SHIMADZU GC-14C instrument equipped with an OV-1701 column with 1,4-dipentyloxy benzene or 1,4-dioctyloxy benzene as the internal reference. Gel-permeation chromatography (GPC) analysis was conducted on a Waters 2414 system equipped with Waters HT4 and HT3 column-assembly and a Waters 2414 refractive index detector (eluent: THF, flow rate: 1.00 ml/min, temperature: 40 °C, standard: polystyrene). Preparative GPC grading of the copolymers was run on a JAI LC-9104 recycling preparative HPLC (JAIGEL 2H/3H column assembly) with toluene as eluent. Matrix-assisted laser desorption ionization time-of-flight (MALDI-TOF) mass spectra were recorded on a Kratos AXIMA-CFR Kompact MALDI Mass Spectrometer with dithranol as the matrix in reflective mode except otherwise noted. UV–vis spectra were obtained on a PerkinElmer Lambda35 UV/Vis Spectrometer. Photoluminescence (PL) spectra were recorded with a PerkinElmer LS50B Luminescence spectrometer. Differential scanning calorimetry (DSC) was performed using a Perkin–Elmer DSC7 at a heating/cooling rate of 10/−10 °C min^{-1} under a nitrogen flow. Tapping-mode atomic force microscopy (AFM) was run on SPA 300HV instrument with an SPI 3800 controller (Seiko Instrument).

2.3. Synthesis of PPP-b-P3HT

Since all diblock copolymerizations were conducted in a similar manner, here only one example was depicted as follows (Scheme 1).

Two Schlenk tubes were thoroughly dried prior to use. In one tube, a mixture of **1** (436 mg, 1.0 mmol), LiCl (42 mg, 1.0 mmol), ^{i}PrMgCl (0.5 mL, 1.0 mmol) and 1,4-dioctyloxybenzene (internal standard for GC analysis, 72 mg, 0.25 mmol) in dry THF (5 mL) was stirred at room temperature for 24 h (solution A). In the other tube, solution B was prepared in the same method with **2** (326 mg, 1.0 mmol), LiCl (42 mg, 1.0 mmol), ^{t}BuMgCl (0.6 mL, 1.0 mmol) and 1,4-dipentyloxybenzene (the internal standard for GC analysis, 63 mg, 0.25 mmol) in THF (8 mL). The solutions A and B of 0.5 and 0.8 mL, respectively, were withdrawn after the magnesium–halogen exchange reactions for GC analysis. Conversions of **1** and **2** were 89% and 96%, respectively. At room temperature, a suspension of Ni(dppe)Cl_2 (15.2 mg, 0.029 mmol) in dry THF (5 mL) was added to the solution A. After stirring for 40 min, 0.6 ml solution was withdrawn for GC and GPC analysis (78% of phenyl Grignard reagent **3** was consumed, M_n and PDI of homopolymer PPP are 5.8×10^3 and 1.23, respectively), then the solution B was added via syringe. After another 40 min (90% of thienyl Grignard reagent **4** was consumed), the polymerization was quenched by addition of 5 M HCl aqueous solution. The mixture was extracted with $CHCl_3$, and the organic extracts were washed with brine, dried over anhydrous $MgSO_4$. After concentrated under reduced pressure, the solution was dropped into methanol for precipitation. The solid was filtered, extracted via a Soxhlet extractor with acetone and then chloroform as the solvents. Finally, chloroform was removed by evaporation to give PPP-*b*-P3HT ($M_n = 1.2 \times 10^4$, PDI = 1.17) as a dark brown solid (203 mg, 53%). According to the amount of the catalyst and the conversions of the magnesium–halogen exchange and polymerization, the numbers of phenylene and thiophene units, *m* and *n*, in the diblock copolymer were calculated to be 22 and 29 (*m*:*n* = 43:57), respectively. ^{1}H NMR (300 MHz, $CDCl_3$) δ = 7.19–7.04 (m, Ph-***H***), 7.00–6.90 (m, Th-***H***), 4.10–3.85 (m, Ph-OC***H***$_2$$C_5H_{11}$), 2.83–2.59 (m, Th-C***H***$_2$$C_5H_{11}$), 1.71–1.66 (m, Ph-OCH$_2$C***H***$_2$$C_4H_9$ + Th-CH$_2$C***H***$_2$$C_4H_9$), 1.44–1.27 (m, Ph-O$C_2H_4C_3$***H***$_6$$CH_3$ and Th-$C_2H_4C_3$***H***$_6$$CH_3$), 0.94–0.85 (m, Ph-O$C_5H_{10}$C***H***$_3$ and Th-C_5H_{10}C***H***$_3$). The ratio of PPP:P3HT estimated from ^{1}H NMR is 43:57.

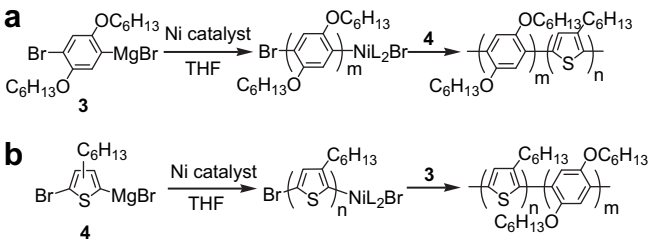

Scheme 1. Synthesis of diblock copolymers PPP-*b*-P3HTs with the monomer addition in the order of **3** and then **4** (a), and **4** and then **3** (b). L in the scheme stands for ligand. Ni catalyst is Ni(dppe)Cl_2 or Ni(dppp)Cl_2, dppp = 1,3-bis(diphenylphosphino) propane; dppe = 1,2-bis (diphenylphosphino) ethane.

3. Results and discussion

3.1. Synthesis of block copolymers

In Yokozawa's report on PPP-*b*-P3HT, [39] it was found that the order of polymerization was crucial and copolymerization was successful only with the monomer addition order of **3** and then **4**. According to the references, the conditions of the GRIM "quasi-living" polymerizations for PPP and P3HT are different in terms of catalysts and additives [10,14]. The "quasi-living" polymerization of monomer **3** was achieved in presence of LiCl with Ni(dppe)Cl_2 as the catalyst [14], while that of monomer **4** was catalyzed by Ni(dppp)Cl_2 without LiCl [10]. Since copolymerization must be carried out with the same catalyst in the presence of LiCl, it is important to study the polymerization mechanism for both PPP and P3HT in the presence of LiCl to exclude the effect of

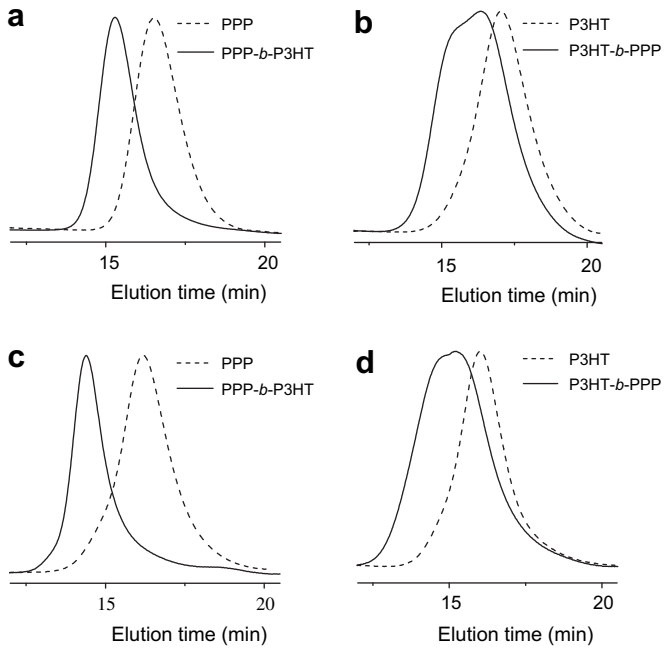

Fig. 1. Gel-permeation chromatography (GPC) elution curves of homopolymer (dash) and copolymerization product (solid) for copolymerizations with equal amount of compounds **1** and **2**, and 1.45 mol% catalyst to the sum of them. (a) Monomer addition order: **3** and then **4**; catalyst: Ni(dppe)Cl_2; PPP: $M_n = 5.8 \times 10^3$, PDI = 1.23; copolymer: $M_n = 1.2 \times 10^4$, PDI = 1.17. (b) Monomer addition order: **4** and then **3**; catalyst: Ni(dppe)Cl_2; P3HT: $M_n = 4.1 \times 10^3$, PDI = 1.33; copolymerization mixture: $M_n = 6.7 \times 10^3$, PDI = 1.44. (c) Monomer addition order: **3** and then **4**; catalyst: Ni(dppp)Cl_2; PPP: $M_n = 5.9 \times 10^3$, PDI = 1.32; copolymer: $M_n = 1.5 \times 10^4$, PDI = 1.22. (d) Monomer addition order: **4** and then **3**; catalyst: Ni(dppp)Cl_2; P3HT: $M_n = 7.0 \times 10^3$, PDI = 1.36; copolymerization mixture: $M_n = 1.1 \times 10^4$, PDI = 1.65.

polymerization condition. As shown in Fig. S1 in supporting information (SI), we found that the polymerization for both PPP and P3HT with either Ni(dppp)Cl_2 or Ni(dppe)Cl_2 as the catalyst in the presence of LiCl followed "quasi-living" mechanism. Therefore in the diblock copolymerization, the magnesium–halogen exchange of **2** and successive polymerization for P3HT block were both carried out in the presence of LiCl, different from previous report in

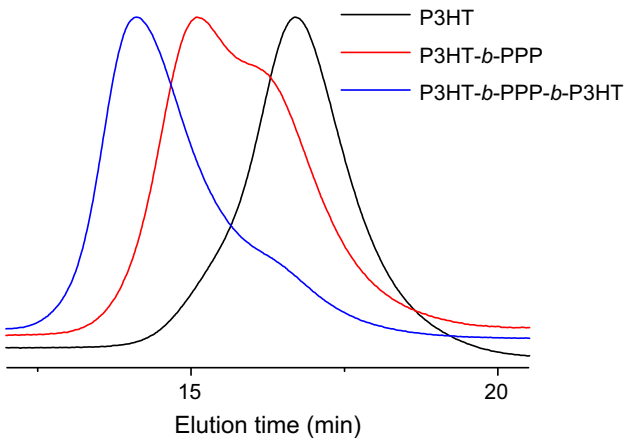

Fig. 2. GPC elution curves of P3HT ($M_n = 4.9 \times 10^3$, PDI = 1.35), diblock copolymerization mixture ($M_n = 8.3 \times 10^3$, PDI = 1.43) and triblock copolymerization mixture ($M_n = 1.5 \times 10^4$, PDI = 1.57). The triblock copolymerization was carried out with the monomer addition in the order of **4**, **3**, and then **4**. The **2**/**1**/**2** feed ratio of 1/1/2 and 4.0 mol% Ni(dppe)Cl_2 to the first portion of **2** were employed.

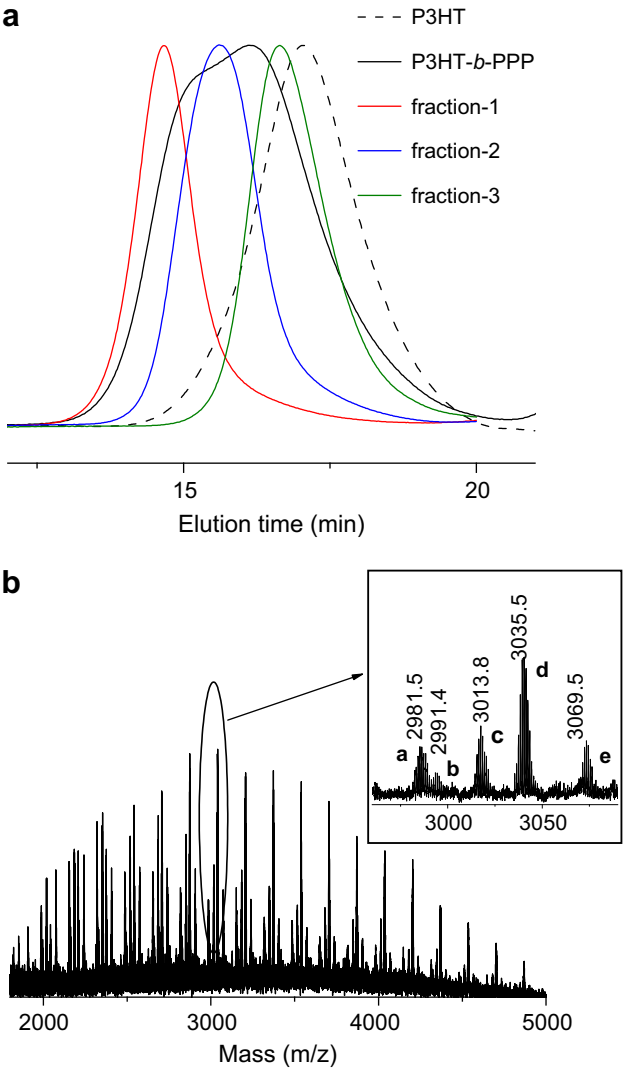

Fig. 3. (a) GPC profiles of P3HT ($M_n = 4.1 \times 10^3$, PDI = 1.33), diblock copolymerization mixture ($M_n = 6.7 \times 10^3$, PDI = 1.44) and its three fractions from preparative GPC separation: fraction-1 ($M_n = 1.4 \times 10^4$, PDI = 1.18), fraction-2 ($M_n = 8.2 \times 10^3$, PDI = 1.19), fraction-3 ($M_n = 4.4 \times 10^3$, PDI = 1.17). (b) MALDI-TOF mass spectrum of the fraction 3. The inset is the expanded spectrum. The copolymerization was carried out with equal amount of compounds **1** and **2**, and 1.45 mol% Ni(dppe)Cl_2 to the sum of them.

which the additive LiCl was not particularly used for P3HT [39]. However, this optimization of polymerization condition again gave the similar results to Yokozawa's report, and the copolymerization was only successful with the order of PPP and then P3HT, as shown in Fig. 1. The GPC elution curves as shown in Fig. 1b and d even show two peaks, probably corresponding to diblock copolymers and "deactivated" polymers. In fact, when we added additional **4** after diblock copolymerization, the peak at longer elution time almost kept unchanged, while the peak at shorter elution time left-shifted, as shown in Fig. 2. Clearly, the two peaks in the GPC profile of the diblock copolymerization product can be ascribed to the active diblock copolymer and "deactivated" polymer, respectively.

To confirm the "deactivation" in the copolymerization with the order of **4** and then **3**, the copolymerization mixture as shown in Fig. 1b was graded into three fractions as shown in Fig. 3a according to elution time by preparative GPC for detail analysis. The fraction 1 is clearly P3HT-*b*-PPP diblock copolymers since its profile almost has no overlap with that of P3HT. The fraction 3 is mainly attributed

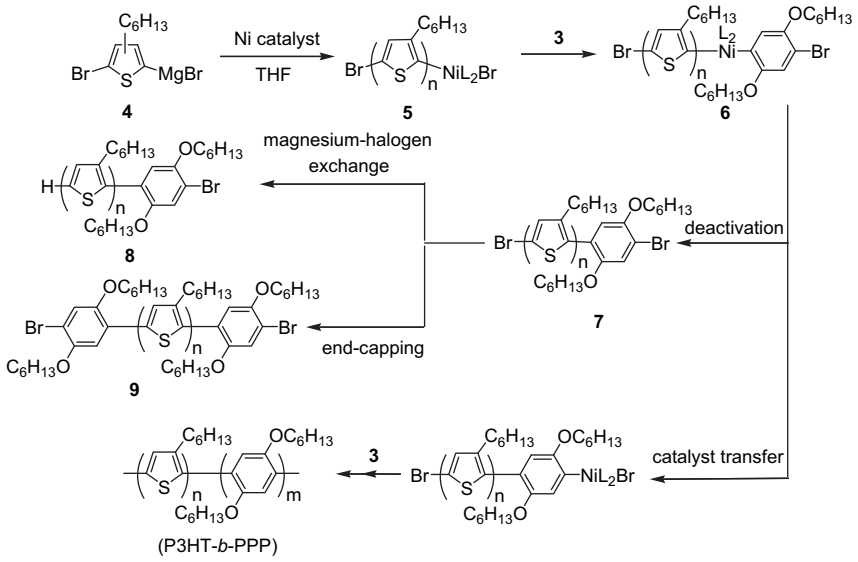

Scheme 2. The proposed "deactivation" pathway of the polymer chains with the monomer addition order of **4** and then **3**.

to the "deactivated" polymers produced in the homopolymerization or at the early period of the copolymerization. Then the composition of this fraction was studied by MALDI-TOF mass spectroscopic technique, and the corresponding spectrum is shown in Fig. 3b. There are five series of peaks in the spectrum, and the difference between the adjacent peaks in the same series is 166 Da, corresponding to one thiophene unit. For easy analysis, the spectrum was expanded with a group of peaks including one from each series, which were marked as a–e as shown in the inset of Fig. 3b. The corresponding monoisotopic masses were also marked in the expanded spectrum. The molecular weight of 2981.5 for the peak *a* is in good agreement with the value calculated by the formula of 166.1 (mass of thiophene unit) × 17 + 78.9 (mass of Br) × 2, corresponding to P3HT with Br/Br ends (BrTh17Br) and 17 thiophene units. Following the similar method, peaks *b* and *e* can be assigned to P3HT (18 repeating units) with H/H and H/Br ends, respectively. These three peaks also appear in MALDI-TOF spectrum of P3HT from homopolymerization of **4** with Ni(dppe)Cl_2 as the catalyst, as shown in Fig. S3 in SI, and may be ascribed to the deactivated P3HT during the homopolymerization, as aforementioned. The peak *d* is the strongest peak in the spectrum, and its molecular weight is consistent with the formula 166.1 × 14 + 78.9 × 2 + 276.2 (mass of phenylene unit) × 2 = 3035.6. Two structures, i. e., BrPhTh14PhBr and BrTh14PhPhBr, are possible. Considering that the intramolecular Ni catalyst transfer in the polymerization for PPP is facile and efficient, this peak should be assigned to double-end-capped product of P3HT with **3**, which is BrPhTh14PhBr. As McCullough reported, P3HT chains can be end-capped at both terminals by using appropriate Grignard reagents [42,43]. The second strongest peak, the peak *c*, corresponds to the molecular mass calculated by 166.1 × 16 + 1.0 (mass of H) + 78.9 + 276.2 = 3013.7, and can be ascribed to HTh16PhBr or BrTh16PhH. We think that the former one is more preferable. Although BrTh16PhH can be afforded by quenching the active chain BrTh16Ph–NiL_2–Br, possibility of this species is low because chain propagation is very fast once the Ni intramolecular transfer occurs, and this active chain should not remain after polymerization of **3** for 40 min. Based on these results, a possible deactivation mechanism is proposed as shown in Scheme 2. Once Grignard reagent **3** is added into the P3HT (**5**) solution, a phenyl unit is coupled to the chain end instantly for yielding the compound **6**. Since thiophene unit is more electron-rich than phenylene unit [39], Ni may prefer interacting with thiophene unit, which significantly slows the intramolecular transfer of Ni toward the chain end, and consequently, chain deactivation via reduction elimination takes place to produce mono-end-capped P3HT (**7**), which can undergo further end-capping reaction as reported by McCullough [42,43] to yield P3HT with BrPh/PhBr ends (**9**), such as BrPhTh14PhBr. P3HT with H/PhBr ends (**8**) is probably originated from the magnesium–halogen exchange between P3HT with Br/PhBr ends (**7**) and **3**.

Following above studies, a series of diblock copolymers, PPP-*b*-P3HTs, with different compositions were synthesized with the

Table 1
Ratios of PPP and P3HT blocks (*m*:*n*), number-average molecular weights (M_ns) and polydisdersity indices (PDIs) of hompolymers PPP and P3HT, and PPP-*b*-P3HT diblock copolymers BmTn, in which *m* and *n* represent the numbers of phenylene and thiophene units.

Entry	Polymer	m[a]	n[a]	m:n[a]	m:n[b]	Homopolymer		Copolymer		Yield[c] (%)
						$M_n \times 10^{-3}$	PDI	$M_n \times 10^{-3}$	PDI	
1	B22T29	22	29	43:57	43:57	5.8	1.23	11.6	1.17	53
2	B9T45	9	45	17:83	16:84	3.1	1.18	10.5	1.19	58
3	B16T44	16	44	27:73	26:74	4.9	1.24	13.8	1.21	65
4	B30T40	30	40	43:57	41:59	8.3	1.24	17.5	1.17	57
5	B69T43	69	43	62:38	64:36	26.0	1.25	32.4	1.30	62
6	PPP	\	\	\	\	11.4	1.26	\	\	68
7	P3HT	\	\	\	\	10.6	1.19	\	\	63

[a] Calculated based-on the ratios of converted monomers/catalyst.
[b] Actual values as calculated according to ^{1}H NMR spectra.
[c] Overall yield based-on the sum of **1** and **2** after Soxhlet extraction with acetone.

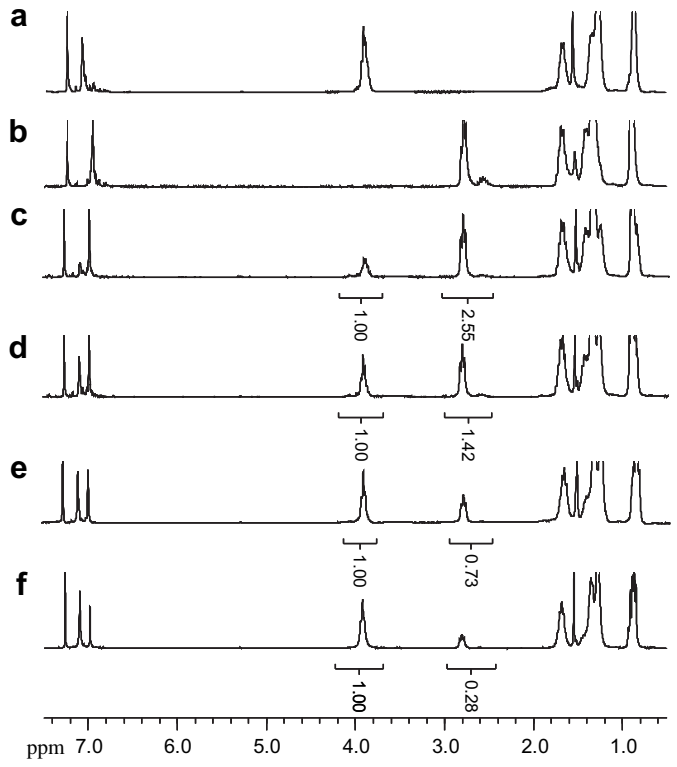

Fig. 4. ^{1}H NMR spectra of (a) PPP (M_n = 1.14 × 10^4, PDI = 1.26), (b) P3HT (M_n = 1.06 × 10^4, PDI = 1.19), (c) B9T45, (d) B16 T44, (e) B30T40 and (f) B69T43 measured in $CDCl_3$ at 20 °C.

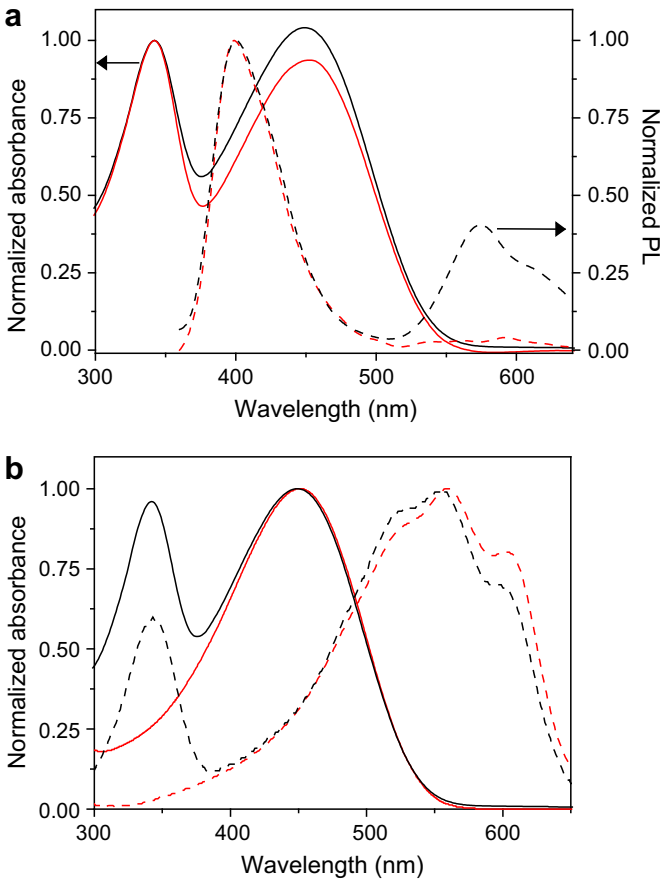

Fig. 5. (a) Solution UV–vis absorption (solid lines) and photoluminescence (PL, dash lines) spectra of the copolymer B30T40 (black lines) and the blend of PPP and P3HT homopolymers (red lines, PPP:P3HT = 41:59). (b) Solution (solid lines) and film (dash lines) UV–vis spectra of the copolymer B30T40 (black) and P3HT homopolymer (red). Solution UV–vis and PL spectra were measured in chloroform with the concentrations of the monomer units of 5.0 × 10^{-5} and 6.0 × 10^{-6} mol/L for absorption and PL measurements, respectively. Films with the thickness of ~25 nm were prepared by spin-casting 5 mg/mL chlorobenzene solution at 1000 rpm on quartz for 60 s. M_n/PDI of B30T40, PPP and P3HT are 1.75 × 10^4/1.17, 1.14 × 10^4/1.26 and 1.06 × 10^4/1.19, respectively. Actual *m*:*n* of PPP and P3HT blocks for B30T40 is 41:59 as measured by ^{1}H NMR.

monomer addition in the order of **3** and then **4** with Ni(dppe)Cl_2 as the catalyst, and M_ns and PDIs of the diblock copolymers are listed in Table 1. M_ns and PDIs of homopolymers PPP and P3HT, which are used as reference polymers, are also included. Fig. 4 shows the ^{1}H NMR spectra of representative PPP-*b*-P3HTs and reference homopolymers. The signals at 4.10–3.85 and 2.83–2.59 ppm are assigned to the methylene protons next to the oxygen in the PPP segment and the methylene protons next to thiophene ring in the P3HT segment, respectively. The actual ratios of phenylene and thiophene units in copolymers (*m*:*n*) can be calculated based on the integral ratios of these two signals. As listed in Table 1, these values (*m*:*n*[b]) are very close to the ones (*m*:*n*[a]) as calculated based on the ratios of converted monomers/catalyst and all copolymers exhibit monomodal GPC profiles with PDI lower than 1.30, indicating that the copolymerizations were well-controlled. Since GPC measurements usually give overestimated molecular weights for conjugated polymers [44–46], we can not calculate the actual numbers of phenylene and thiophene units (m and *n* for phenylene and thiophene, respectively) in the diblock copolymers according to GPC measurements. Approximately, we use *m* and *n* as calculated based-on the ratios of converted monomers/catalyst to name the diblock copolymers as BmTn, in which B and T represent phenylene and thiophene rings, respectively.

3.2. Photophysical properties

Blends of two conjugated polymers and their diblock copolymer counterparts should exhibit distinct photoluminescence (PL) because intramolecular Förster energy transfer is more efficient than intermolecular one. Therefore, the formation of the diblock copolymers can also be supported by comparing the PL spectra of the diblock copolymers and the blends of the related homopolymers in very dilute solution [7]. Here we select one of the PPP-*b*-P3HTs, B30T40, as an example. Homopolymers P3HT and PPP as shown in Table 1 were blended in the *m*:*n* ratio as 41:59, which was the same as the actual ratio of B30T40 as calculated according to ^{1}H NMR spectrum. Fig. 5a shows UV–vis (concentration of the monomer units = 5.0 × 10^{-5} mol/L) and PL (concentration of the monomer units = 6.0 × 10^{-6} mol/L) spectra of the copolymer and

Table 2
Endothermal transition temperatures and corresponding enthalpies of PPP-*b*-P3HT diblock copolymers (BmTn) and homopolymers PPP and P3HT based-on the second DSC heating traces with a heating rate of 10 °C/min under N_2.

Polymer	Endothermal transition temperatures (°C)/enthalpy (J/g)	
	1st peak	2nd peak
B22T29	76.1 (35.5)	196.5 (12.5)
B16T44	67.0 (8.8)	224.5 (17.9)
B9T45	\	220.5 (22.7)
B30T40	83.1 (20.4)	222.3 (13.1)
B69T43	96.6 (36.6)[a]	231.0 (7.8)
PPP[b]	96.1 (66.0)	\
P3HT[c]	\	214.6 (14.9)

[a] There is an exothermal transition peak at 67.4 °C (−23.0 J/g).
[b] M_n and PDI are 1.14 × 10^4 and 1.26, respectively.
[c] M_n and PDI are 1.06 × 10^4 and 1.19, respectively.

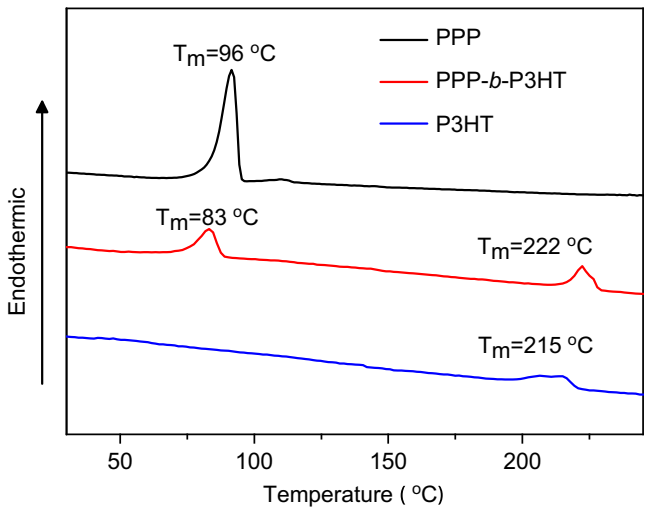

Fig. 6. The second heating DSC traces of the diblock copolymer B30T40 and homopolymers PPP and P3HT at a heating rate of 10 °C/min in N_2. M_n/PDI of B30T40, PPP and P3HT are 1.75×10^4/1.17, 1.14×10^4/1.26 and 1.06×10^4/1.19, respectively. Actual *m*:*n* of PPP and P3HT blocks for B30T40 is 41:59 as measured by ^{1}H NMR.

the blend in dilute chloroform solution. In PL measurements, the excitation wavelength was fixed at 340 nm, which is the absorption maximum of PPP. It is clear that their PL spectra are quite different, although UV–vis spectra are identical. For the copolymer, significant energy transfer from the PPP block to the P3HT block was observed, indicated by presence of pronounced emission of P3HT at around 580 nm. In contrast, very weak emission from P3HT for the blend was observed because the distance was too far for efficient energy transfer between PPP and P3HT in a very dilute solution.

Fig. 5b shows film UV–vis absorption spectra of the copolymer B30T40 and P3HT with a film thickness of ~25 nm. Compared with solution ones, the P3HT related bands of the copolymer are bathochromically shifted over 100 nm, like the behavior of the homopolymer P3HT. This indicates that the copolymer can also form the film comprising highly ordered P3HT blocks [47].

3.3. Thermal properties

The phase transition temperatures of copolymers were measured by DSC in nitrogen atmosphere, and the related data are listed in Table 2. Typical DSC scans are depicted in Fig. 6 with B30T40 as an example. DSC scans of PPP and P3HT homopolymers

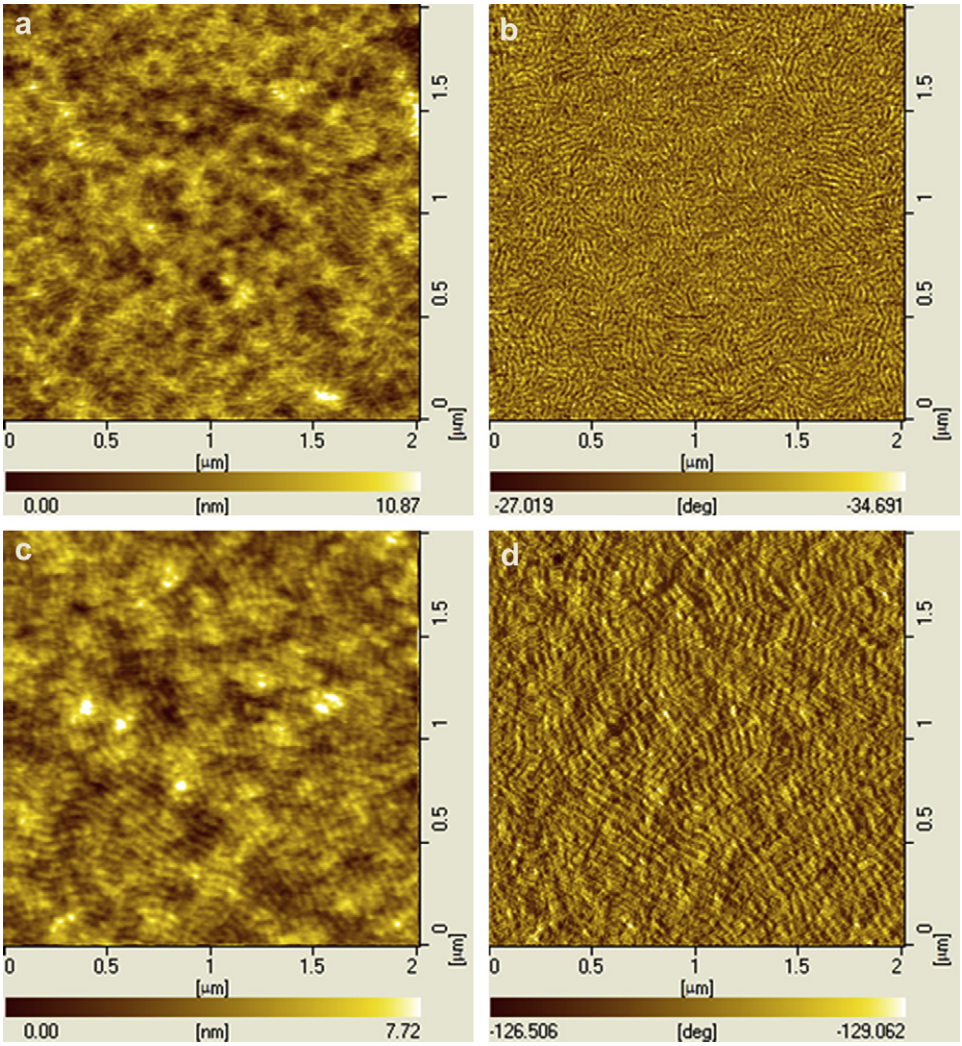

Fig. 7. Atomic force microscopy (AFM) topography (a and c) and phase (b and d) images of a thin film of B30T40 ($M_n = 1.75 \times 10^4$; PDI = 1.17; *m*:*n* = 41:59) (a and b) and B69T43 ($M_n = 3.24 \times 10^4$; PDI = 1.30; *m*:*n* = 64:38) (c and d) after holding at 105 °C for 30 min and quenched in liquid nitrogen. The film with the thickness of ~30 nm was prepared by spin-casting 5 mg/mL chlorobenzene at 1000 rpm on SiO_2 substrates.

are also included for comparison. The copolymer exhibits two phase transitions at 83.1 and 222.3 °C, which can be ascribed to the melting of PPP and P3HT blocks, respectively, by comparing DSC scans of the copolymer and the homopolymers. From Table 2, all copolymers have two endothermal transitions except B9T45, which has the shortest PPP block and only shows one transition for P3HT block. These results clearly indicate the emergence of the microphase separation between PPP and P3HT blocks in the copolymers.

To further confirm the microphase separation of the diblock copolymers, thin films of the copolymers B30T40 and B69T43 were spin coated from 5 mg/mL chlorobenzene solutions on SiO_2 substrates and quenched from 100 °C. Their morphologies were characterized with atomic force microscopy (AFM). As shown in Fig. 7, the films clearly exhibit phase separated morphologies, and the phase images show lamellar morphologies. Noticeably, the periods of the lamellar are around 25 and 42 nm for B30T40 and B69T43, respectively, which are close to the chain lengths of the two copolymers. This indicates that film morphology can be tuned by modulation of the chain lengths and compositions of PPP-*b*-P3HT diblock copolymers. Comparing with crystalline-amorphous diblock architecture, all-conjugated diblock copolymers comprising crystalline–crystalline blocks may have unique optoelectronic properties [38].

4. Conclusion

A series of all-conjugated PPP-*b*-P3HT diblock copolymers with different block ratios were synthesized by "quasi-living" Grignard metathesis (GRIM) polymerization. Mass spectroscopic analysis indicates that the effect of the addition order of the monomers on copolymerization is attributed to the low efficiency of intramolecular Ni transfer from thiophene to phenylene units. All diblock copolymers except one with the shortest PPP block exhibit two endothermal transitions corresponding to the melting of PPP and P3HT blocks, respectively, indicative of crystalline–crystalline nature and microphase separation characteristic of the diblock copolymers. The formation of microphase-separated nanostructures was also supported by AFM observations.

Acknowledgment

This work is supported by National Basic Research Program of China (973 Project, No. 2009CB623603) of Chinese Ministry of Science and Technology, NSFC (Nos. 20521415, 20621401 and 50833004).

Appendix. Supporting information

Details for homopolymerizations and triblock copolymerization, MALDI-TOF mass spectra for P3HT homopolymers with different catalysts are provided as supplementary material. Supplementary data associated with this article can be found in the online version, at doi:10.1016/j.polymer.2009.11.001.

References

[1] (a) Thompson BC, Fréchet JMJ. Angew Chem Int Ed 2008;47:58; (b) Günes S, Neugebauer H, Sariciftci NS. Chem Rev 2007;107:1324.
[2] Grimsdale AC, Chan KL, Martin RE, Jokisz PG, Holmes AB. Chem Rev 2009;109:897.
[3] Allard S, Forster M, Souharce B, Thiem H, Scherf U. Angew Chem Int Ed 2008;47:4070.
[4] Hoeben FJM, Jonkheijm P, Meijer EW, Schenning APHJ. Chem Rev 2005;105:1491.
[5] Schwartz BJ. Ann Rev Phys Chem 2003;54:141.
[6] Lee M, Cho B-K, Zin W-C. Chem Rev 2001;101:3869.
[7] Scherf U, Gutacker A, Koenen N. Acc Chem Res 2008;41:1086.
[8] Yokozawa T, Yokoyama A. Prog Polym Sci 2007;32:147.
[9] Yokoyama A, Yokozawa T. Macromolecules 2007;40:4093.
[10] Iovu MC, Sheina EE, Gil RR, McCullough RD. Macromolecules 2005;38:8649.
[11] Miyakoshi R, Yokoyama A, Yokozawa T. J Am Chem Soc 2005;127:17542.
[12] Adachi I, Miyakoshi R, Yokoyama A, Yokozawa T. Macromolecules 2006;39:7793.
[13] Vallat P, Lamps J-P, Schosseler F, Rawiso M, Catala J-M. Macromolecules 2007;40:2600.
[14] Miyakoshi R, Shimono K, Yokoyama A, Yokozawa T. J Am Chem Soc 2006;128:16012.
[15] Huang L, Wu SP, Qu Y, Geng YH, Wang FS. Macromolecules 2008;41:8944.
[16] Stefan MC, Javier AE, Osaka I, McCullough RD. Macromolecules 2009;42:30.
[17] Yokoyama A, Kato A, Miyakoshi R, Yokozawa T. Macromolecules 2008;41:7271.
[18] Senkovskyy V, Khanduyeva N, Komber H, Oertel U, Stamm M, Kuckling D, et al. J Am Chem Soc 2007;129:6626.
[19] Khanduyeva N, Senkovskyy V, Beryozkina T, Bocharova V, Simon F, Nitschke M, et al. Macromolecules 2008;41:7383.
[20] Khanduyeva N, Senkovskyy V, Beryozkina T, Horecha M, Stamm M, Uhrich C, et al. J Am Chem Soc 2009;131:153.
[21] Urien M, Erothu H, Cloutet E, Hiorns RC, Vignau L, Cramail H. Macromolecules 2008;41:7033.
[22] Higashihara T, Ohshimizu K, Hirao A, Ueda M. Macromolecules 2008;41:9505.
[23] Radano CP, Scherman OA, Stingelin-Stutzmann N, Müller C, Breiby DW, Smith P, et al. J Am Chem Soc 2005;127:12502.
[24] Boudouris BW, Frisbie CD, Hillmyer MA. Macromolecules 2008;41:67.
[25] Dai C-A, Yen W-C, Lee Y-H, Ho C-C, Su W-F. J Am Chem Soc 2007;129:11036.
[26] Iovu MC, Jeffries-El M, Sheina EE, Cooper JR, McCullough RD. Polymer 2005;46:8582.
[27] Iovu MC, Jeffries-El M, Zhang R, Kowalewski T, McCullough RD. J Macromol Sci Part A 2006;43:1991.
[28] Sauvé G, McCullough RD. Adv Mater 2007;19:1822.
[29] Craley CR, Zhang R, Kowalewski T, McCullough RD, Stefan MC. Macromol Rapid Commun 2009;30:11.
[30] Iovu MC, Craley CR, Jeffries-El M, Krankowski AB, Zhang R, Kowalewski T, et al. Macromolecules 2007;40:4733.
[31] Richard F, Brochon C, Leclerc N, Eckhardt D, Heiser T, Hadziioannou G. Macromol Rapid Commun 2008;29:885.
[32] Zhang QL, Cirpan A, Russell TP, Emrick T. Macromolecules 2009;42:1079.
[33] Yokozawa T, Adachi I, Miyakoshi R, Yokoyama A. High Perform Polym 2007;19:684–99.
[34] Zhang Y, Tajima K, Hirota K, Hashimoto K. J Am Chem Soc 2008;130:7812.
[35] Ohshimizu K, Ueda M. Macromolecules 2008;41:5289.
[36] Benanti TL, Kalaydjian A, Venkataraman D. Macromolecules 2008;41:8312.
[37] Ouhib F, Khoukh A, Ledeuil J-B, Martinez H, Desbrières J, Dagron-Lartigau C. Macromolecules 2008;41:9736.
[38] Wu P-T, Ren GQ, Li CX, Mezzenga R, Jenekhe SA. Macromolecules 2009;42:2317.
[39] Miyakoshi R, Yokoyama A, Yokozawa T. Chem Lett 2008;37:1022.
[40] Jammi S, Rout L, Punniyamurthy T. Tetrahedron: Asymmetry 2007;18:2016.
[41] Lüttringhaus A. Liebigs Ann Chem 1937;528:181.
[42] Jeffries-El M, Sauvé G, McCullough RD. Adv Mater 2004;16:1017.
[43] Jeffries-El M, Sauvé G, McCullough RD. Macromolecules 2005;38:10346.
[44] Liu Q, Liu WM, Yao B, Tian HK, Xie ZY, Geng YH, et al. Macromolecules 2007;40:1851.
[45] Zhang XJ, Qu Y, Bu LJ, Tian HK, Zhang JP, Wang LX, et al. Chem Eur J 2007;13:6238.
[46] Liu Q, Qu Y, Geng YH, Wang FS. Macromolecules 2008;41:5964.
[47] Faï K, Fréchette M, Ranger M, Mazerolle L, Levesque I, Léclerc M, et al. Chem Mater 1995;7:1390.